

Original Research Article

Sustainable Synthesis of Cobalt Nanoparticles from Temple Waste flowers of Pink Rose, Red Rose, Yellow Rose and Orange Rose Petals Extracts

Boorasamy Dhinakaran^{1*} , S. Monika¹, S. Nivetha¹, M. Shalini¹, B. Vishnupriya¹, Kaliyan Sathiyamoorthi² 

¹PG and Research Department of Physics, Government Arts College, Chidambaram –608 001, Tamilnadu, India

²PG and Research Department of Chemistry, Government Arts College, Chidambaram – 608 001, Tamilnadu, India

ARTICLE INFORMATION

Received: 14 January 2023

Received in revised: 25 February 2023

Accepted: 02 March 2023

Available online: 08 March 2023

DOI: 10.26655/AJNANOMAT.2023.1.4

KEYWORDS

Sustainable synthesis

Temple waste

Cobalt nanoparticles

Nano-Plant biotechnology

Characterization

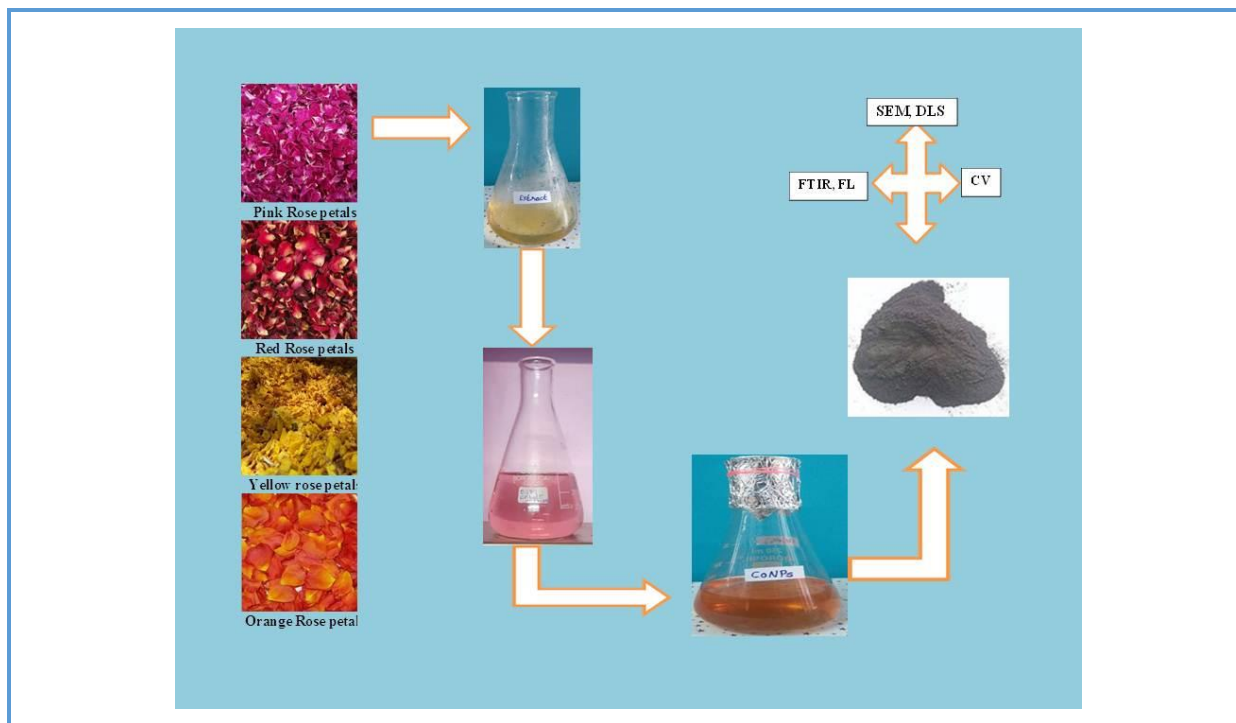
Electrochemical properties

ABSTRACT

Sustainable synthesis of metallic nanoparticles has ensnared the world from the chemical and physical slants owing to its rapid, harmless, and pecuniary trait of production mechanism. The present study demonstrates green synthesis of CoONPs using petal extract of temple wastes of pink rose (ROR), red rose (RER), yellow rose (YOR), and orange roses (ORR). To date, there is no report on the synthesis of CoONPs utilizing an aqueous flower extract of these four rose petals. In this research work, four rose flowers petal extract in a concentrated solution of cobalt nitrate hexahydrate in CoONPs. Cobalt nitrate hexa hydrate was reserved as the metal precursor, whereas flower extract act as a reducing and stabilizing agent. The phytochemicals present in the extract act as reducing agents, which include saponins, phenolic compounds, and flavonoids. Phyto-constituents and CoONPs stretching and bending vibration are measured by FTIR spectroscopy, FL spectrum was also done to study the fluorescence activity of cobalt nanoparticles with four different rose petal extracts, Morphology of the cobalt nanoparticles were designed by scanning electron microscope (SEM), and the particle size are measured by dynamic light scattering (DLS) analysis. Finally, the electrochemical properties of CoONPs were studied by cyclic voltammetry (CV) with impedance spectrum.

© 2023 by SPC (Sami Publishing Company), Asian Journal of Nanoscience and Materials, Reproduction is permitted for noncommercial purposes.

Graphical Abstract



Introduction

Flowers come as waste from several cradles like celebration halls, hotels, gardens, churches, dargahs, temples, marriages, funeral rites, and different other cultural ceremonies of religious, [Figure 1\(a-d\)](#) shows floral waste in various places. In India, religion is a path of life. It is an intrinsic element of the entire Indian culture. People adore God and are familiar with going to the shrines and offering flowers, fruits, coconuts, milk, and sweets. The bulk of the flowers, leaves of different plants, coconut shells, milk, and curd are piled up and then inclined entirely in water bodies [\[1\]](#). Every day, these flowers are accessible by aficionados in temples and are left unexploited and therefore become leftovers. India is a country of jubilees, and many junctures are celebrated around the year, eventually leading to solid waste generation. This fraction of waste is mainly mistreated and entails due contemplation. Because of our spiritual dogmas, many of us

avoid hurling flowers and other items used for supplications in the garbage. Instead, we put them in plastic bags and throw them directly in the water bodies. Apart from this, flowers are also kept under the sacred trees, and thus there is no suitable mode of disposal. Degradation of floral waste is a prolonged process compared to kitchen waste degradation [\[2\]](#).

This floral waste can be befittingly proficient and exploited in innumerable value-added forms. Techniques like vermicomposting, Incense sticks, dye extraction, essential oils, making of colors, and bio-gas generation can be used. Most flowers comprise secondary metabolites, which can be further used in food additives. Flowers contain various coloring materials like dyes. Dyes are very long and complicated organic structures; these compounds are converted to metal nanoparticles to develop a new biotechnological route and improve the nanoparticle bids. Some flower extracts

mediated nanoparticle synthesis are listed in [Table 1](#).

Co_3O_4 NPs attracted numerous research interests due to their low cost and good electrochemical. Conversely, cobalt is a d-block metal capable of exhibiting several possible oxidation states (Co^{2+} , Co^{3+} , and Co^{4+}) because this transition metal has three unpaired electrons in ground state configuration and also release the valence electron to appear with various positive charge or various oxidation state. Co_3O_4 is a known multi-functional, anti-ferromagnetic p-type semi-conductor with a spinel crystal structure [3]. The direct optical band gaps of Co_3O_4 NPs were about 1.48 and 2.19 eV [4], and it can be used as a photocatalyst

to vitiate several organic contaminants by visible light. Cobalt can be found in different spin states in its oxide forms, such as low, high, and intermediate spin. These spin circumstances kind the physics of the Co_3O_4 gorgeous from a necessary viewpoint and in spintronic applications. Hence, Co_3O_4 NPs novelties have massive applications in extents such as arena influence transistor, energy storage [5], catalysis [6], anode material in Li-ion rechargeable batteries [7], electrochromic sensors [8], solar cells [9] and photocatalyst [10]. In addition, Co_3O_4 NPs have antioxidant, antifungal, antibacterial, anticancer, and enzyme inhibition properties due to their superior biomedical applications [11-12].



Figure 1. (a) Collection of flower wastes, (b) Flower waste disposed in river water and banks, (c) Flower waste in Funeral rites, (d) Flower disposed in Temple pond as waste

Table 1. Shows the flower-mediated nanoparticle synthesis

S.No	Flower species	Metal nanoparticles	Reference
1	<i>Rosa floribunda charisma</i>	Magnesium nanoparticles	Younis,2021[13]
2	<i>Rosmarinus o_cinalis L.</i>	Magnesium nanoparticles	Abdallah, 2019[14]
3	Rose (Rosa sp.) petals	Gold Nanoparticles	Jha, 2013[15]
4	<i>Lablab purpureus</i>	Silver Nanoparticles	Muruganantham,2018 [16]
5	<i>Gnidia glauca</i>	Gold Nanoparticles	Ghosh, 2012[17]
6	<i>Hibiscus rosa-sinensis</i>	Silver Nanoparticles	Nayak,2015[18]
7	<i>Chrysanthemum indicum L.</i>	Silver Nanoparticles	Arokiyaraj, 2015[19]
8	<i>Ipomoea digitata Linn.</i>	Silver Nanoparticles	Venkatesan,2019[20]
9	Marigold flower	Silver Nanoparticles	Padalia,2014[21]
10	<i>Caesalpinia pulcherrima</i>	Silver Nanoparticles	Moteriya,2016[22]
11	<i>Nyctanthes arbor-tristis</i>	Zinc oxide Nanoparticles	Jamdagni, 2016[23]
12	<i>Mimusops elengi</i>	Copper Nanoparticles	Sarah, 2019[24]
13	<i>Syzygium aromaticum</i>	Zinc oxide Nanoparticles	Lakshmeesha, 2019[25]
14	<i>Jacaranda mimosifolia</i>	Zinc oxide Nanoparticles	Sharma, 2016[26]
15	<i>Piliostigma thonningii</i>	Iron Nanoparticles	Igwe, 2018[27]
16	Marigold (<i>Tagetes sp.</i>) and Rose (<i>Rosa sp.</i>)	Cadmium nanoparticles	Hajra,2016[28]

Materials and Methods

Sample collection

Flower wastes collected from Sri Nataraja temple, Chidambaram, Cuddalore district, Tamilnadu, India. The collected wastes were separated by hand picking method. The collection of four types of waste rose petals is shown in Figure 2. The roses were separated

from the waste collections and then washed three times in running tap water to remove dust particles attached within and three times in double distilled water. Then the washed roses were dried at room temperature for five to six days and ground well until turn into powder using a pestle and mortar. This powder was collected in airtight glass tube used for preparation of extract.



Pink Rose petals



Red Rose petals



Yellow rose petals



Orange Rose petals

Figure 2. Image of dried Roses petals of different colors

Chemicals, Solvents and Starting Materials

De-ionized water, whatman 1 μ and whatman 41 μ filter papers, Potassium di chromate Ethyl alcohol, Sodium hydroxide pellets, Hydrochloric acids, Sulphuric acid, and other chemicals were purchased from Merck (India) Ltd. All the chemicals were used without further purification.

Instruments and equipment

Electric oven, Magnetic stirrer (REMI 2 MLH), E-1 portable TDS and EC meter, pH-009(I)A pen-type pH meter, sterilized separating funnels (250 mL), sterilized conical flasks (500 mL), sterilized beakers (400 mL), watch glasses, funnels (7"), 10 mL measuring cylinders and glass rods.

Extraction

5 grams of each rose powder was taken in four separate 250 mL round bottom flasks in which 50 ml of double distilled water (DDW) was poured. The water condenser was fitted and fixed with the running tap water, then heated for 20 min at 80 °C. Then the extracts were filtered through whatman 1 μ filter paper,

and the filtrates were used for the further green synthesis.

Green synthesis of cobalt nanoparticle from Rose flower extract

A cobalt nitrate solution of 0.1 mM was prepared. To this drop by drop 10 mL of rose flower petal extract has been added. The color changes were observed after 30 min. Adding 1M NaOH solution checks and adjusts the pH to 12. Dispersing in sterile purified water and centrifuged for 30 min at 700 rpm three times. The particles with black color were subsequently washed with double distilled water to remove the impurities from the final products [29]. Then it was dried by vacuum oven at 60 °C for 6 h to obtain a bluish block crystal. The green synthesized cobalt nanoparticles have been characterized by UV, FL, FTIR, DLS, and SEM and also carried out by cyclic voltammetry analysis used to measure the reduction potential of the green synthesized cobalt nanoparticles (CoNPs) Figure 3 (a-c). Similar processes were followed for the other three rose petal extract-mediated cobalt oxide nanoparticle synthesis.



Figure 3. (a) Extract of rose petal, (b) 0.1 M cobalt nitrate solution, (c) CoNPs suspension

Result and Discussion

Characterization

Co₃O₄ nanoparticles were characterized by diverse techniques, for instance, Fluorescence properties studies by Fluorescence spectroscopy (FL), FTIR (400–4000 cm⁻¹) spectroscopy analysis by various phytochemical constituents of the cobalt nanoparticles with four different rose petal extracts. Another analysis method is by dynamic light scattering (DLS) to measure the average size of the cobalt nanoparticles. Morphology and shape were studied via SEM analysis. Cyclic voltammetry was carried out using an electrochemical analyzer (CHI760C) to study the oxidation state of metal ions in a potential range of -2 to 2V. Calomel (Hg/Hg₂Cl₂), glassy carbon, and platinum wire served as reference, working, and counter electrodes, respectively.

FTIR Spectral analysis

The FTIR spectrum of CoNPs obtained was carried out to identify the possible biomolecules responsible for capping and efficient stabilization of CoNPs synthesis is using pink rose (*Rosa sp.*) petal extract. The FTIR spectrum of pink rose (*Rosa sp.*) petal capped CoNPs, showed absorptions at 3448.99 cm⁻¹ due to -OH group of polyphenolic compounds, the frequency of 2924.37 cm⁻¹ have shown in -NH group of amine and amide compounds, aromatic C=C have shown in 2426.45 cm⁻¹, carbonyl group contain acetamide group have shown in 1633.75 cm⁻¹, and the strong peak of 1384.30 cm⁻¹ have revealed that -O-H bending vibration for Hydroxyl group contain phyto-constituent and cobalt hydroxide, The vibration peak of 516.47 cm⁻¹ have been indicating the Co-O vibrational stretching (Figure 4). The existence of phenolic compounds and proteins

was assured by the functional vibrations bands group as demonstrated in the FTIR spectrum. All these confirm that water-soluble phytochemicals present in the Rose (*Rosa sp.*) petal extract has the aptitude to accomplish twin utilities of lessening and calming the cobalt nanoparticles

The FTIR spectrum of a red rose (*Rosa sp.*) petal-capped CoNPs, showed absorptions at 3444.34 cm⁻¹ due to -OH group of polyphenolic compounds. The frequency of 2923.32 cm⁻¹ have shown in -NH group of amine and amide compounds, aromatic C=C have shown in 2853.05 cm⁻¹, carbonyl group containing acetamide group have shown in 1632.75 cm⁻¹, the strong peak of 1384.30 cm⁻¹ have reveals that -O-H bending vibration for Hydroxyl group contain phyto-constituent and cobalt hydroxide, The vibration peak of 517.23 cm⁻¹ have been indicating the Co-O vibrational stretching. Figure 5, The functional vibrations groups assured the existence of phenolic compounds and proteins as demonstrated in the FTIR spectrum. All these confirm that water-soluble phytochemicals contemporary in the red rose (*Rosa sp.*) petal extract can achieve dual purposes of reduction and stabilization of the cobalt nanoparticles. The FTIR spectrum of yellow Rose (*Rosa sp.*) petal-capped CoNPs, showed absorptions at 3451.86 cm⁻¹ due to -OH group of polyphenolic compounds. The frequency of 2428.47 cm⁻¹ has shown in -NH group of amine and amide compounds, aromatic C=C have shown in 2093.18 cm⁻¹, Carbonyl group containing acetamide group have shown in 1630.52 cm⁻¹. The strong peak of 1384.30 cm⁻¹ has revealed that -O-H bending vibration for the hydroxyl group contains phyto-constituent and cobalt hydroxide. The vibration peak of 517.47 cm⁻¹ has indicated the Co-O vibrational stretching (Figure 6). The existence of phenolic compounds and proteins was assured by the functional vibrations groups

as demonstrated in the FTIR spectrum. All these confirm that water-soluble phytochemicals present in the yellow rose (*Rosa sp.*) petal extract can perform twin functions of reduction and stabilization of the cobalt nanoparticles. The FTIR spectrum of orange rose (*Rosa sp.*) petal-capped CoNPs showed absorptions at 3448.60 cm^{-1} due to -OH group of polyphenolic compounds. The frequency of 2925.44 cm^{-1} has shown in -NH group of amine and amide compounds, aromatic C=C have shown in 2426.45 cm^{-1} , carbonyl group containing the acetamide group have shown in 1627.86 cm^{-1} . The strong peak of 1384.30 cm^{-1} revealed that -

O-H bending vibration for the hydroxyl group contains phyto-constituent and cobalt hydroxide, The vibration of 1068.30 cm^{-1} has shown in C-C-C bending. The vibration peak of 517.32 cm^{-1} indicate the Co-O vibrational stretching (Figure 7). The functional vibrations groups' existence of phenolic compounds and proteins was assured by the functional vibrations groups as demonstrated in the FTIR spectrum. All these confirm that water-soluble phytochemicals present in the Orange Rose (*Rosa sp.*) petal extract can perform dual functions of reduction and stabilization of the cobalt nanoparticles.

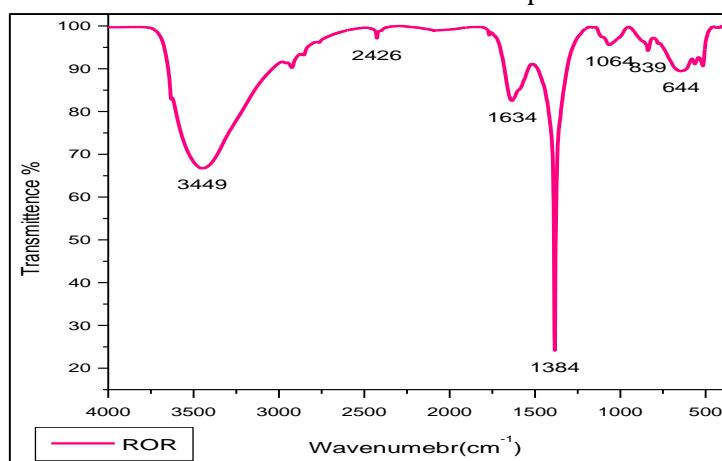


Figure 4. FTIR spectrum of Pink Rose petal extract mediated cobalt nanoparticles

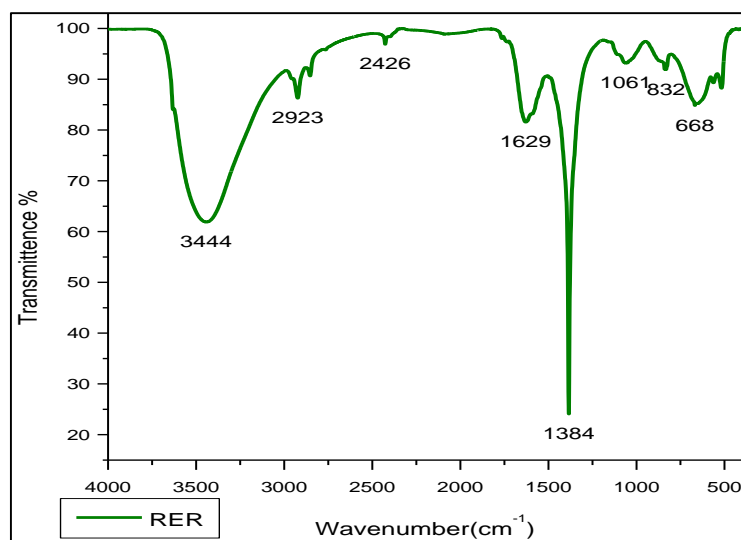


Figure 5. FTIR spectrum of Red Rose petal extract mediated cobalt nanoparticles

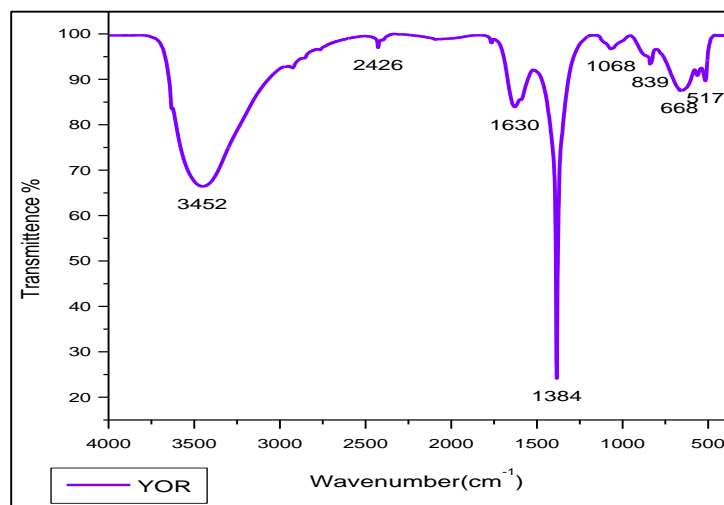


Figure 6. FTIR spectrum of Yellow Rose petal extract mediated cobalt nanoparticles

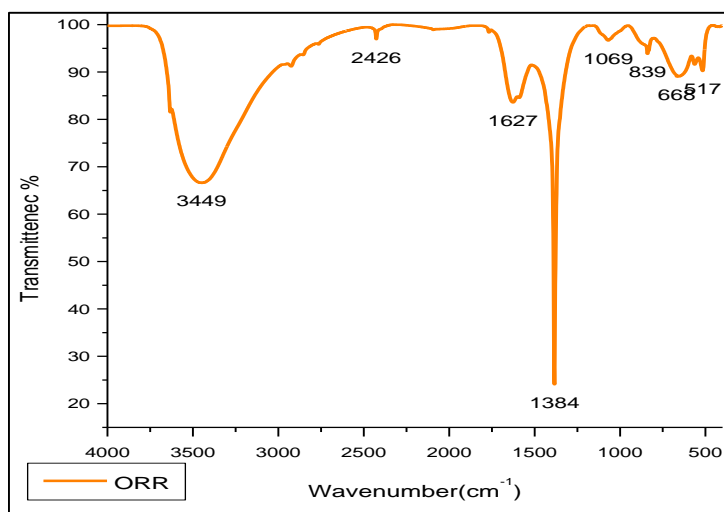


Figure 7. FTIR spectrum of Orange Rose petal extract mediated cobalt nanoparticles

Fluorescence spectral analysis

Figure 8 shows the fluorescence excitation and emission spectra for cobalt nanoparticles, respectively. The excitation wavelength was fixed at 900 nm, and the emission spectra were recorded for the green synthesized cobalt nanoparticles, which are water-based cobalt nanoparticles. Cobalt nanoparticles by pink rose (ROR) in water showed two fluorescence emissions at 725.44 nm & fluorescence intensity (FI) at 208.72 and 437.55 nm and FI:

24.74. Cobalt nanoparticles by red rose (RER) in water showed two fluorescence emissions at 725.57 nm & fluorescence intensity (FI) at 251.07 and 438.01 nm & FI: 24.41. Cobalt nanoparticles by yellow rose (YOR) in water showed two fluorescence emissions at 725.50 nm and fluorescence intensity (FI) at 308.75 and 440.86 nm and FI: 30.61. Cobalt nanoparticles by orange rose (ORR) in water showed two fluorescence emissions at 725.65 nm and fluorescence intensity (FI) at 274.75 and 442.12 nm and FI: 24.08. The cobalt

nanoparticles of four rose petals mediated green synthesis are shown two peaks, one present in the blue shift, other peak shown in redshift region. Pink rose-mediated cobalt nanoparticles were shown to have a lower fluorescence wavelength, and yellow rose rose-

mediated cobalt nanoparticles had a higher fluorescence wavelength. Comparing the four cobalt nanoparticles, yellow rose petals extract-mediated cobalt nanoparticles have a higher fluorescence effect.

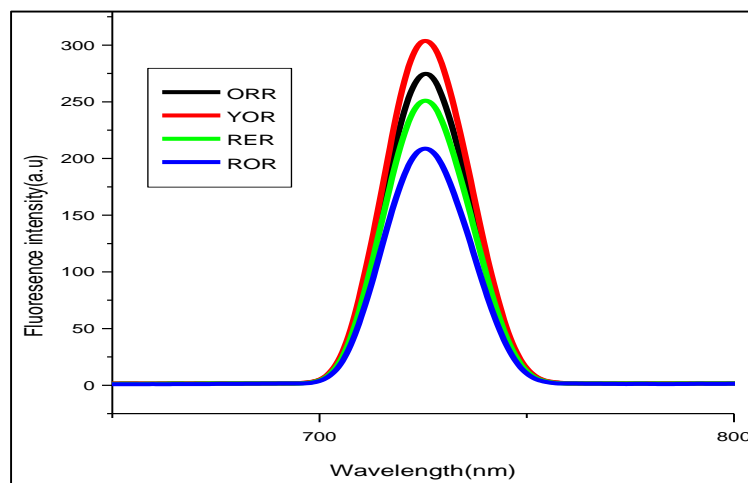


Figure 8. FL spectrum of Cobalt nanoparticles mediated by aqueous extract of Pink, Red, Yellow, and Orange rose petals

DLS Analysis

Particle size distributions have been made using dynamic light scattering where He – Ne laser light (633 nm) is passed through diluted nanoparticle solutions. The size distributions of cobalt nanoparticles mediated by an aqueous extract of pink, red, yellow, and orange rose petals are shown in [Figure 9](#). X-Axis shows the particle size in μm with a logarithmic scale. Cobalt nanoparticle sizes ranging from 2 nm to 95 nm with 20 to 70 nm distribution were obtained.

SEM Analysis

The scanning electron microscopic analysis ([Figures 10-13](#)) was employed to identify the morphologies (shape) of the synthesized cobalt nanoparticles mediated by four different rose petals and aqueous extracts. SEM images of

cobalt nanoparticles mediated by pink rose petals extracts were [Figure 10a](#) ($2 \mu\text{m}$) confirmed shiny spherical minute granular morphology, [Figure 10b](#) ($1 \mu\text{m}$), adapted by a merged form of cobalt nanoparticles. [Figure 10c](#) ($2 \mu\text{m}$) well-defined by rock-shaped nanoparticles, [Figure 11](#) shows the SEM images of cobalt nanoparticles mediated by Red rose petal extracts. [Figure 11a](#) shows in cubic crystalline shapes ($2 \mu\text{m}$) and little rod shapes. [Figure 12](#) established the presence of metal CoNPs. The SEM images of cobalt nanoparticles by Yellow rose petals extract displayed cubic, triangular and irregular shapes. The size of nanoparticles is very minute and ranges from $1 \mu\text{m}$ ([12b & c](#)) to $2 \mu\text{m}$ ([12a](#)). [Figure 13](#) reveals the SEM images of cobalt nanoparticles mediated by orange rose petals extracts and shown well-defined cubic, triangular, rocky-shaped nanoparticles. The size displayed by the nanoparticles in [Figure 13 a, b, c](#) are $1 \mu\text{m}$.

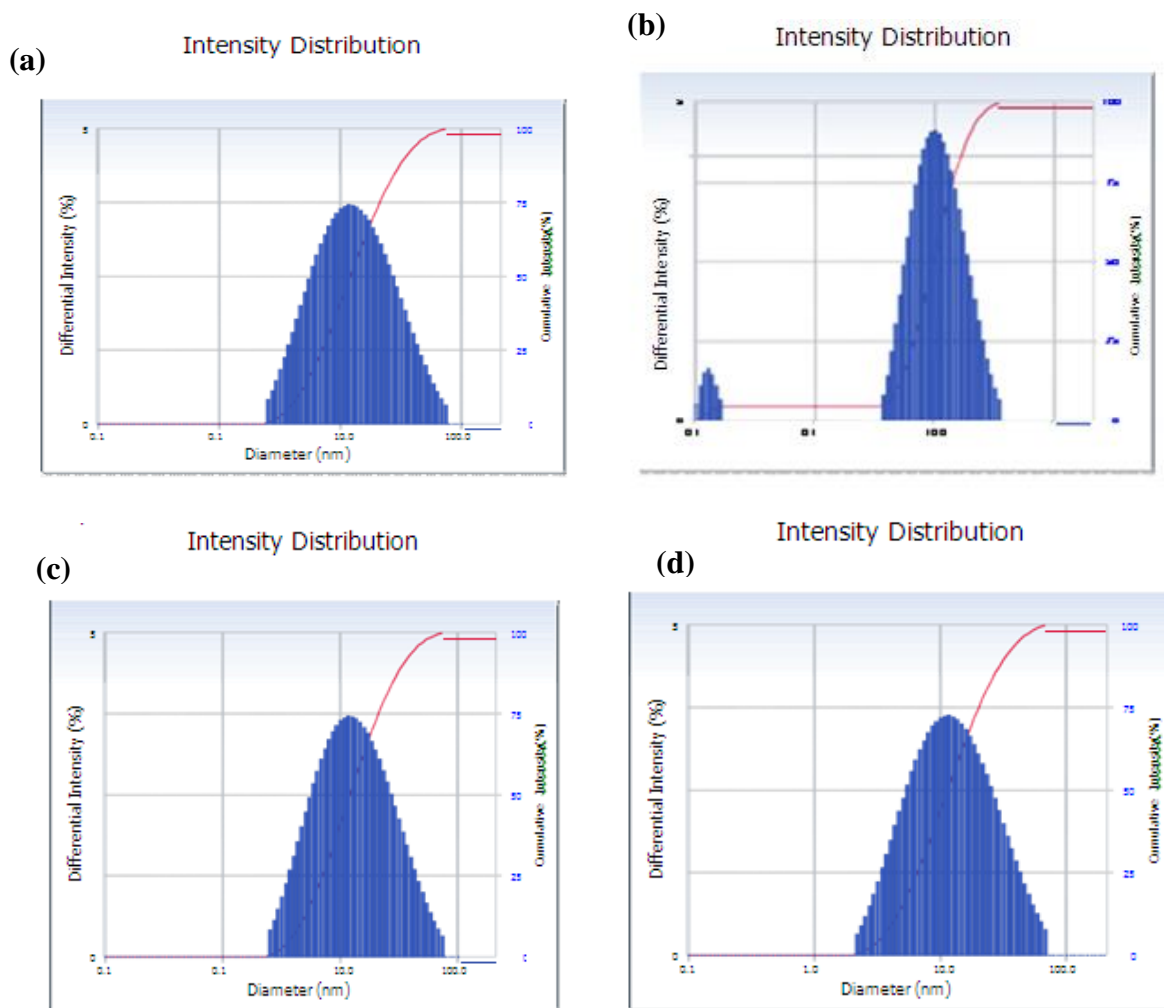


Figure 9. DLS Particle distribution images of Cobalt nanoparticles mediated by aqueous extract of Pink (9a), Red(9b), Yellow(9c), and Orange (9d) rose petals

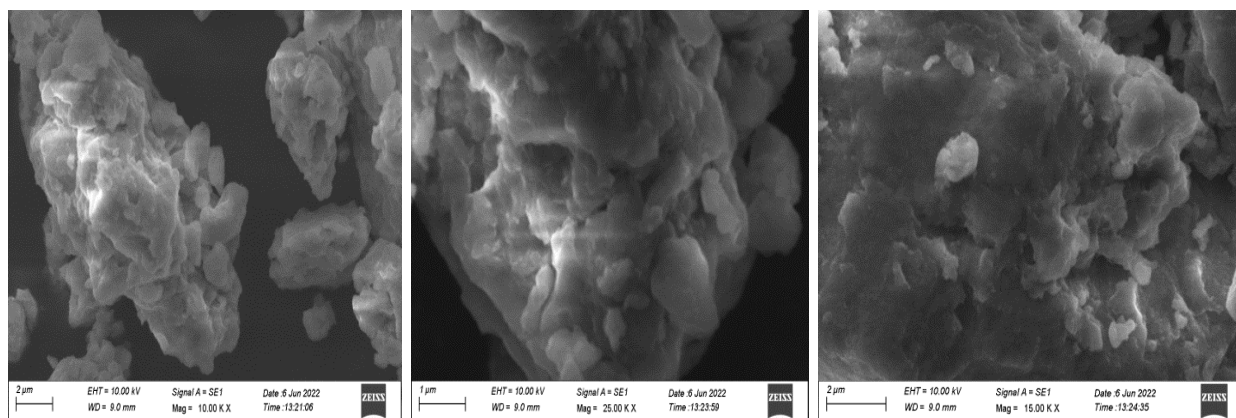


Figure 10. SEM images of cobalt nanoparticles mediated by Pink Rose petal extract

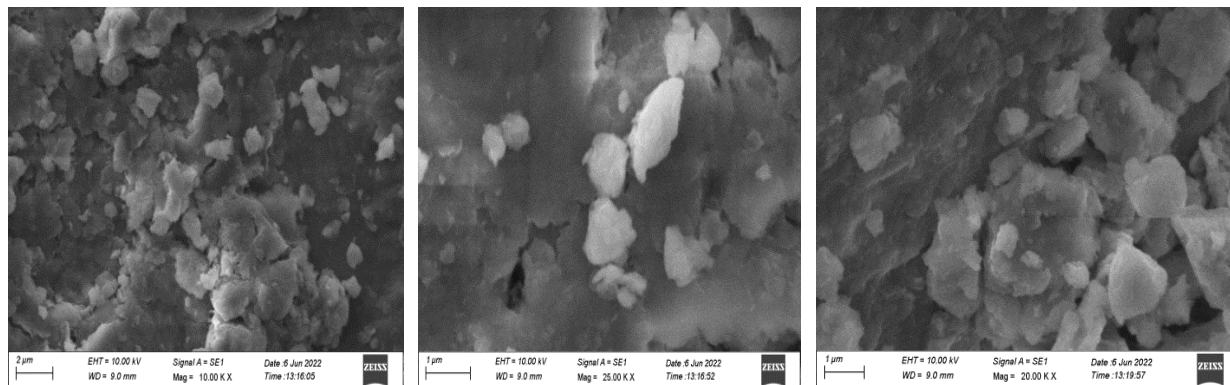


Figure 11. SEM images of cobalt nanoparticles mediated by Red Rose petal extract

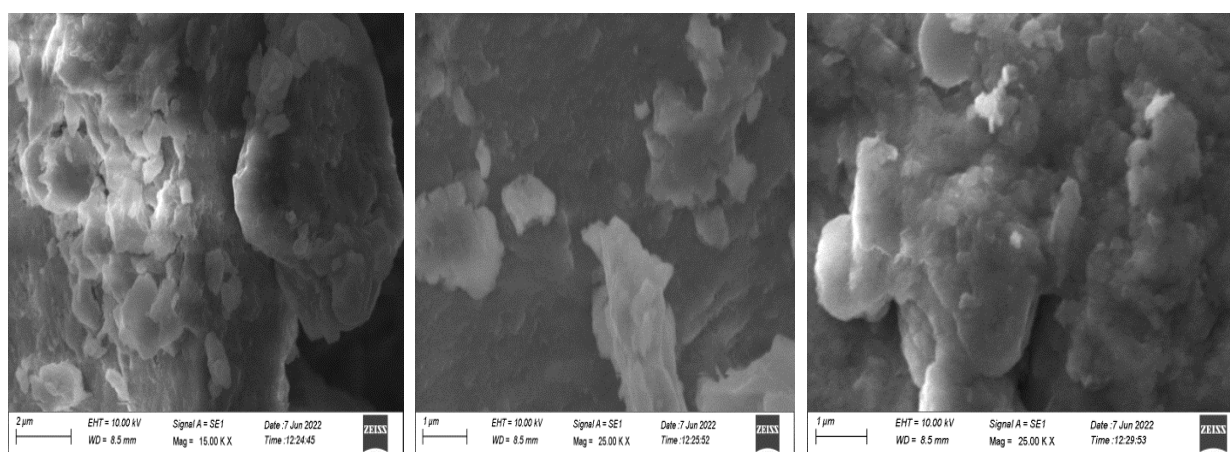


Figure 12. SEM images of cobalt nanoparticles mediated by Yellow Rose petal extract

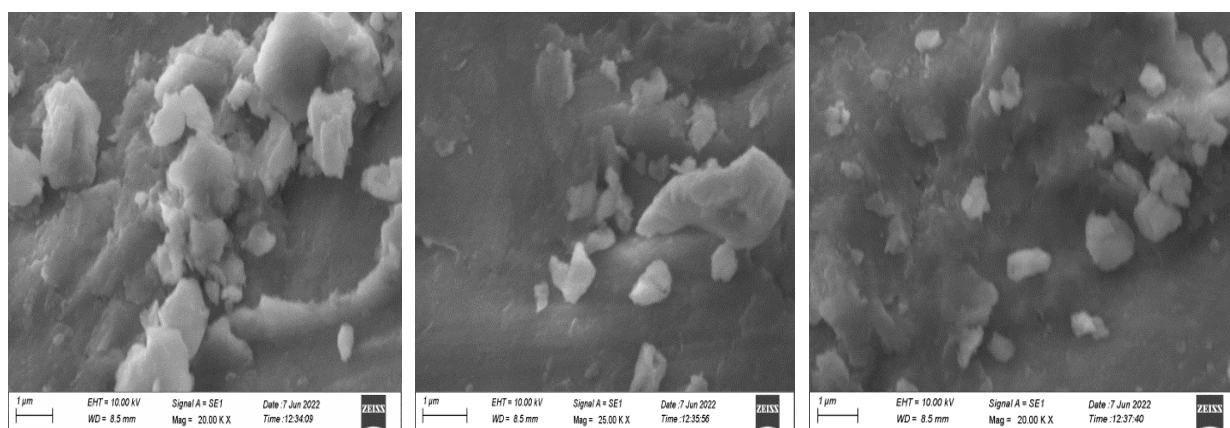


Figure 13. SEM images of cobalt nanoparticles mediated by Orange Rose petal extract

Super-capacitor performance studies

The electrochemical behavior [30-31] of nanoparticles of cobalt oxides mediated by pink

rose, red rose, yellow rose, and orange rose petal extracts were studied. The CV obtained pink rose-mediated cobalt nanoparticles (Figure 14a) shows a single well-defined redox

couple with formal potential, $E^{o'} = (E_{pa} + E_{pc})/2$, of 940 mV vs. SCE in standard buffer (pH = 7) as supporting electrolyte. The peak is not affected by the stirring of the electrolyte, offering proof that the material is well associated with the electrode surface under the solution conditions. Cyclic voltammograms of the cobalt oxide by pink rose petals extracts at different potential scan rates, 716.1 mV to 1.2 V vs. SCE in the standard buffer as supporting electrolyte, were studied. The anodic and cathodic peak current

of the voltammograms is linearly proportional to the square root of scan rate from 300 up to 800 mV s⁻¹, and the ratio i_{pa}/i_{pc} remains almost equal to unity, as expected for a surface-type behavior, which is expected for a diffusion-controlled electrode process. It seems the oxidation of Co (II) possibly creates Co (III) in an alkaline solution, and the oxidation of Co (III) to Co (IV) oxide species occurred during the positive scan in a buffer as a supporting solution.

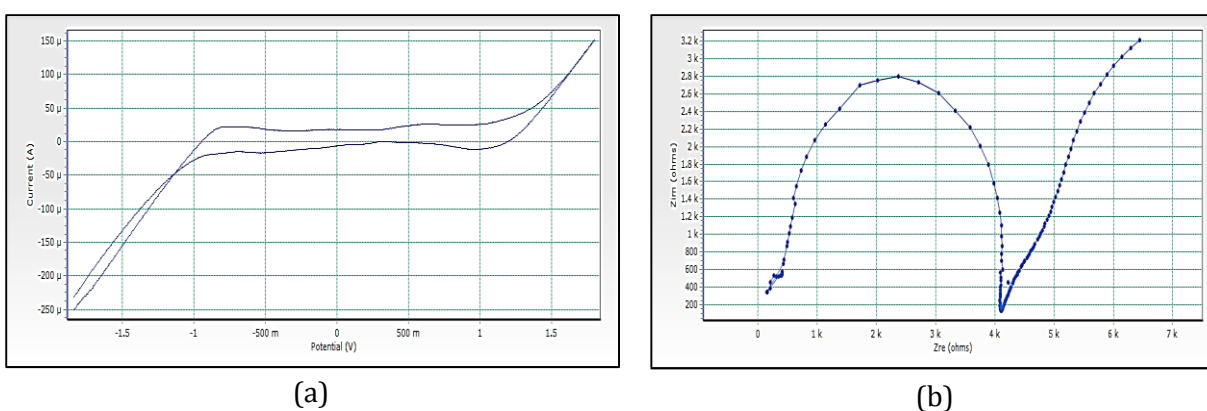


Figure 14. (a) Cyclic voltammograms of cobalt nanoparticles by Pink rose petals extracts, (b) Impedance spectrum of cobalt nanoparticles by Pink rose petals extracts

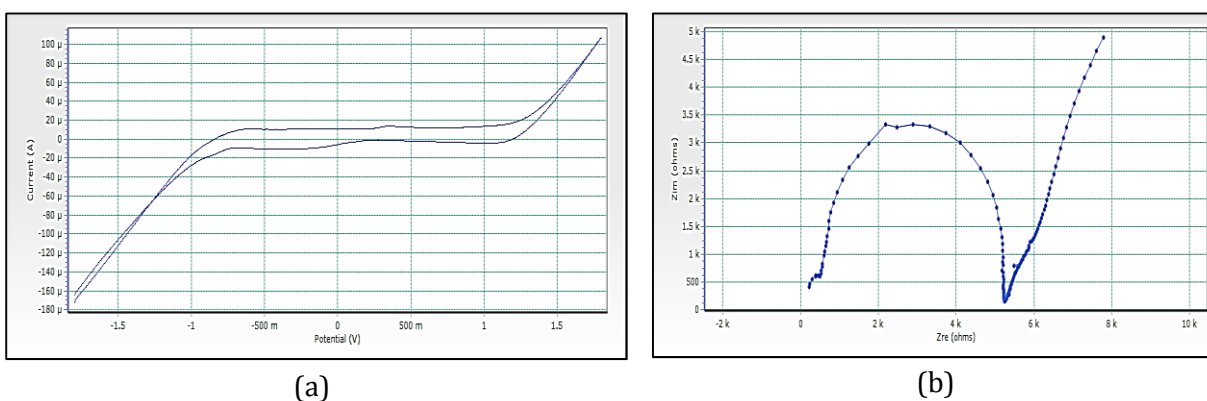


Figure 15. (a) Cyclic voltammograms of cobalt nanoparticles by Red rose petals extracts, (b) Impedance spectrum of cobalt nanoparticles by Red rose petals extracts

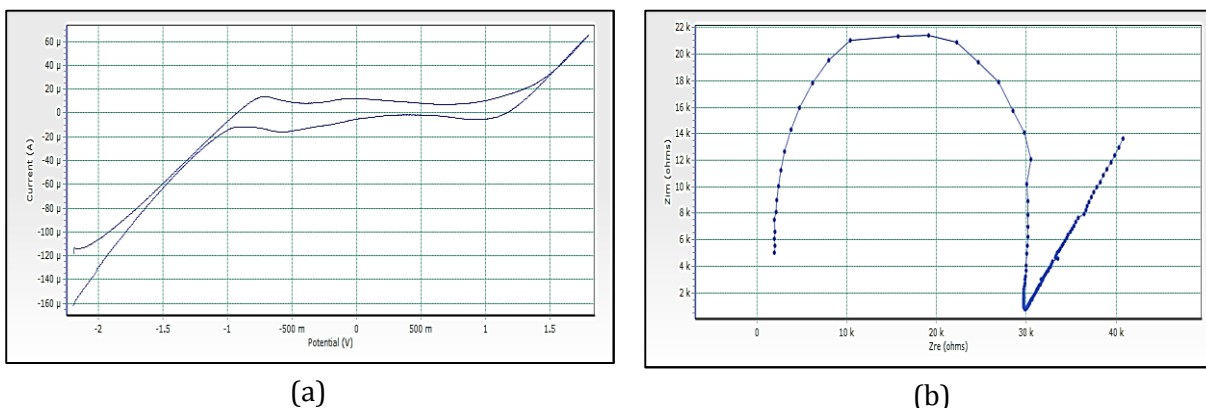


Figure 16. (a) Cyclic voltammograms of cobalt nanoparticles by Yellow rose petals extracts, (b) Impedance spectrum of cobalt nanoparticles by Yellow rose petals extracts

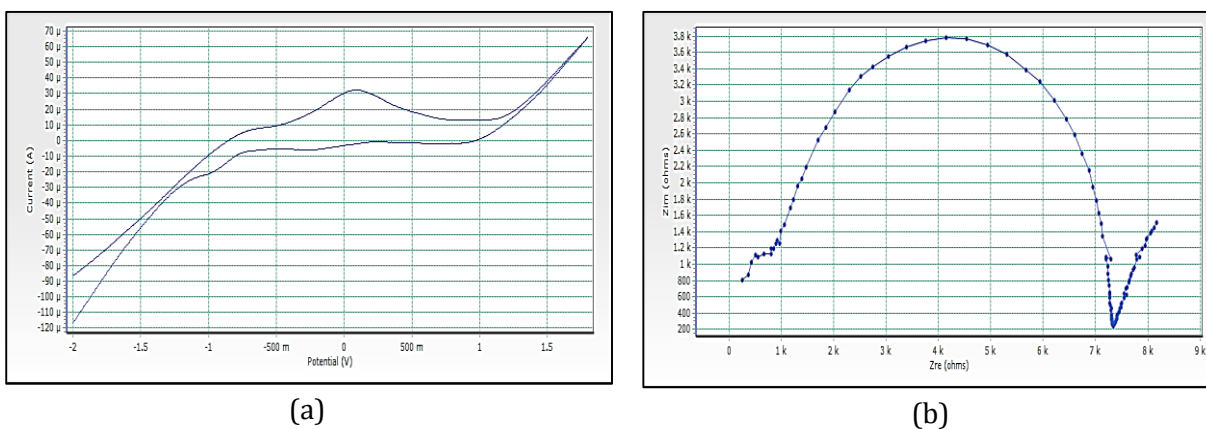


Figure 17. (a) Cyclic voltammograms of cobalt nanoparticles by orange rose petals extracts, (b) Impedance spectrum of cobalt nanoparticles by orange rose petals extracts

Figure 15a reveals the CV of red rose-mediated cobalt nanoparticles. The peak range is -592.5 mV to 83.7 mV, peak area is 123.116 μC , Figure 16a, have shown CV of yellow rose-mediated cobalt nanoparticles, and the peak range is -770.4 mV to -126.9 mV, peak area is 103.324 μC , Figure 17a, have shown CV of yellow rose mediated cobalt nanoparticles and the peak range is -375.7 mV to 551.7 mV, peak area is 348.016 μC . All the result of voltammograms of Cobalt nanoparticles electrode in the presence of pink rose, red rose, yellow rose, and orange rose petal extracts have shown in Table 2. The impedance spectrum (Figure 14b) of cobalt nanoparticles by pink rose petals is shown in 19 points with 24.994

sample deviation, depression is -36.412° , Figure 15b reveals that 27 points with 27.196 sample deviation, depression is -29.116° , Yellow rose petals mediated cobalt nanoparticles are shown in Figure 16b, is evident that strong sample deviation (332.06) comparing with other three cobalt nanoparticles samples. The total points is 22, and the depression is -33.907° . Orange rose-mediated cobalt nanoparticles were shown in a diameter of 6178.5, total point 27, sample deviation of 26.634, and depression is -12.913° . All the result of circle fit results of impedance spectrum in cobalt nanoparticles electrode by pink rose, red rose, yellow rose, and orange rose petal extract have shown in Table 3. Comparing four CV and impedance spectrum of cobalt

nanoparticles was evident that the yellow rose petals mediated cobalt nanoparticles were shown in lower peak area and impedance spectrum also shown higher diameter and higher sample deviations. The electron transfer rate constant (k_s) and the transfer coefficient (α) can be determined by measuring the

variations of peak potentials with a scan rate based on the method described by Laviron [32]. He has derived general expressions for the linear potential sweep voltammetry response for the case of surface-confined electroactive species.

Table 2. Result of voltammograms of Cobalt nanoparticles electrode in the presence of Pink Rose, Red Rose, Yellow Rose and Orange Rose Petal extracts

CoNPs	Peak Analysis				Peak I (μ A)	Peak E (mV)	Area (μ C)	Range
	X ₁ (mV)	Y ₁ (A)	X ₂ (V)	Y ₂ (A)				
Pink rose	716.159	0 A	1.255	0 A	-12.092	944.655	132.98	716.1 mV to 1.2 V
Red Rose	-592.556	-3.543 μ A	83.731	-3.543 μ A	-7.327	-423.867	123.12	-592.5 mV to 83.7 mV
Yellow rose	-770.446	-8.247 μ A	-126.976 mV	-8.247 μ A	-7.844	-574.46	103.32	-770.4 mV to -126.9mV
Orange rose	-375.715	12.62 μ A	551.764 mV	12.62 μ A	19.62	89.558	348.02	-375.7 mV to 551.7 mV

Table 3. Circle Fit Results of Impedance spectrum in Cobalt nanoparticles electrode by Pink Rose, Red Rose, Yellow Rose, and Orange Rose Petal extracts

CoNPs	Center Point X	Center Point Y	Diameter:	Total Points	Sample Deviation	Depression
Pink rose	2335.8	1031.6	3475.7	19	24.994	-36.412°
Red Rose	2926.7	1092.4	4490.2	27	27.196	-29.116°
Yellow rose	16379	7917	28384	22	332.06	-33.907°
Orange rose	4173.8	690.37	6178.5	27	26.634	-12.913°

Conclusion

In the present work, we have synthesized, CoNPs from pink rose, red rose, yellow rose, and orange rose petals extracts. The phytochemicals in the petals acted as reducing and stabilizing agents for forming CoNPs. The sustainable synthesized nanoparticles were round or spherical in shape with an average size of 20-40 nm. The fluorescence spectrum of yellow rose-mediated cobalt nanoparticles is shown in higher fluorescence intensity than the other

three cobalt nanoparticles. CV and impedance spectrum studies also have shown that yellow rose mediated cobalt nanoparticles have different results than other threes. From the study, it is understood that the flowers used in the temple are generally discarded as waste into the environment. It can be utilized to synthesize CoNPs, which can be therapeutically used to control many diseases, especially infectious, stress-related, and cancer. The synthesized CoNPs are a good source of natural antimicrobial, antioxidant, and anticancer

agents. To understand the molecular mechanism *in vivo* studies are needed.

Acknowledgments

The authors would like to acknowledge the Archbishop Casimir Instrumentation Centre (ACIC) St. Joseph's College (Autonomous), Tiruchirappalli-620 002. For performing UV, FTIR, FL, DLS, SEM and CV studies. The authors are also thankful to the Department of Physics, Government Arts College, Chidambaram. For providing laboratorial facilities.

Disclosure Statement

No potential conflict of interest was reported by the authors.

Orcid

B. Dhinakaran : [0000-0002-8431-030X](https://orcid.org/0000-0002-8431-030X)

K. Sathiyamoorthi : [0000-0002-0937-6595](https://orcid.org/0000-0002-0937-6595)

References

- [1]. Lee Y.J., Song K., Cha S.H., Cho S., Kim Y.S., Park Y. *Nanomaterials*, 2019, **9**:819 [[CrossRef](#)], [[Google Scholar](#)], [[Publisher](#)]
- [2]. Shete R.C., Fernandes P.R., Borhade B.R., Pawar A.A., Sonawane M.C., Warude N.S. *J. Chem. Rev.*, 2022, **4**:331 [[CrossRef](#)], [[Publisher](#)]
- [3]. Stella C., Soundararajan N., Ramachandran K. *AIP Adv.*, 2015, **5**:087104 [[Crossref](#)], [[Google Scholar](#)], [[Publisher](#)]
- [4]. Varghese B., Teo C.H., Zhu Y., Reddy M.V., Chowdari B.V., Wee A.T.S., Sow C.H. *Adv. Funct. Mater.*, 2007, **17**:1932 [[Crossref](#)], [[Google Scholar](#)], [[Publisher](#)]
- [5]. Shinde V.R., Mahadik S.B., Gujar T.P., Lokhande C.D. *Appl. Surf. Sci.*, 2006, **252**:7487 [[Crossref](#)], [[Google Scholar](#)], [[Publisher](#)]
- [6]. Sivachidambaram M., Vijaya J.J., Kaviyarasu K., Kennedy L.J., Al-Lohedan H.A., Ramalingam R.J., *RSC Adv.*, 2017, **7**:38861 [[Crossref](#)], [[Google Scholar](#)], [[Publisher](#)]
- [7]. Li W.Y., Xu L.N., Chen J., *Adv. Funct. Mater.*, 2005, **15**:851 [[Crossref](#)], [[Google Scholar](#)], [[Publisher](#)]
- [8]. Han L., Yang D.P., Liu A. *Biosens. Bioelectron.*, 2015, **63**:145 [[Crossref](#)], [[Google Scholar](#)], [[Publisher](#)]
- [9]. Sharma J.K., Srivastava P., Singh G., Akhtar M.S., Ameen S. *Mater. Sci. Eng.: B*, 2015, **193**:181 [[Crossref](#)], [[Google Scholar](#)], [[Publisher](#)]
- [10]. Dewi N.O.M., Yulizar Y., Apriandanu D.O.B., *Green synthesis of Co₃O₄ nanoparticles using Euphorbia heterophylla L. leaves extract: characterization and photocatalytic activity*. In IOP Conference Series: Materials Science and Engineering, 2019, **509**:012105. [[Crossref](#)], [[Google Scholar](#)], [[Publisher](#)]
- [11]. Khalil A.T., Ovais M., Ullah I., Ali M., Shinwari Z.K., Maaza M. *Arab. J. Chem.* 2017, **13**:606 [[Crossref](#)], [[Google Scholar](#)], [[Publisher](#)]
- [12]. Anuradha C.T., Raji P. *Mater. Res. Express*, 2019, **6**:095063 [[Crossref](#)], [[Google Scholar](#)], [[Publisher](#)]
- [13]. Younis I.Y., El-Hawary S.S., Eldahshan O. A., Abdel-Aziz M.M., Ali Z.Y. *Sci. Rep.* 2021, **11**:16868., [[Crossref](#)], [[Google Scholar](#)], [[Publisher](#)]
- [14]. Abdallah Y., Ogunyemi S.O., Abdelazez A., Zhang M., Hong X., Ibrahim E., Hossain A., Fouad H., Li B., Chen J. *BioMed. Res. Int.*, 2019, **2019**:5620989 [[Crossref](#)], [[Google Scholar](#)], [[Publisher](#)]
- [15]. Jha A.K., Prasad K. *J. Bionanosci.*, 2013, **7**:245 [[Crossref](#)], [[Google Scholar](#)], [[Publisher](#)]
- [16]. Muruganantham N., Govindharaju R., Anitha P., Anusuya V.. *Int. J. Sci. Res. Biol. Sci.*, 2018, **5**:1 [[Crossref](#)], [[Google Scholar](#)], [[Publisher](#)]

- [17]. Ghosh S., Patil S., Ahire M., Kitture R., Gurav D.D., Jabgunde A.M., Kale S., Pardesi K., Shinde V., Bellare J. *J. Nanobiotechnol.*, 2012, **10**:17 [[Crossref](#)], [[Google Scholar](#)], [[Publisher](#)]
- [18]. Nayak D., Ashe S., Rauta P.R., Nayak B. *IET Nanobiotechnol.*, 2015, **9**:288 [[Crossref](#)], [[Google Scholar](#)], [[Publisher](#)]
- [19]. Arokiyaraj S., Kumar V.D., Elakya V., Kamala T., Park S.K., Saravanan M., Bououdina M., Arasu M.V., Kovendan K., Vincent S. *Environ. Sci. Pollut. Res.*, 2015, **22**:9759 [[Crossref](#)], [[Google Scholar](#)], [[Publisher](#)]
- [20]. Varadavenkatesan T., Selvaraj R., Vinayagam R. *Int. J. Environ. Sci. Tec.*, 2019, **16**:2395 [[Crossref](#)], [[Google Scholar](#)], [[Publisher](#)]
- [21]. Padalia H., Moteriya P., Chanda S. *Arab. J. Chem.*, 2014, **8**:732 [[Crossref](#)], [[Google Scholar](#)], [[Publisher](#)]
- [22]. Moteriya P., Chanda S. *Artif. Cells Nanomed. Biotechnol.*, (2016) **45**:1556 [[Crossref](#)], [[Google Scholar](#)], [[Publisher](#)]
- [23]. Jamdagni P., Khatri P., Rana J.S. *J. King Saud. Univ. Sci.* 2016, **30**:168 [[Crossref](#)], [[Google Scholar](#)], [[Publisher](#)]
- [24]. Sarah S.L.R., Iyer P.R. *Int. J.Recent. Sci. Res.*, 2019, **10**:32956 [[Google Scholar](#)],
- [25]. Lakshmeesha T.R., Kalagatur N.K., Mudili V., Mohan C.D., Rangappa S., Prasad B.D., Ashwini B.S., Hashem A., Alqarawi A.A., Malik J.A. *Front. Microbiol.*, 2019, **10**:1244 [[Crossref](#)], [[Google Scholar](#)] [[Publisher](#)]
- [26]. Sharma D., Sabela M.I., Kanchi S., Mdluli, P.S., Singh G., Stenström T.A., Bisetty K. *J. Photochem. Photobiol. B: Biol.*, 2016, **162**:199 [[Crossref](#)], [[Google Scholar](#)] , [[Publisher](#)]
- [27]. Hasanpour F., Taei M., Fouladgar M., Salehi M. *J. Appl. Organomet. Chem.*, 2022, **2**:203 [[Crossref](#)], [[Google Scholar](#)], [[Publisher](#)]
- [28]. Hajra A., Dutta S., Mondal N.K. *J. Parasit. Dis.*, 2016, **40**:1519 [[Crossref](#)], [[Google Scholar](#)], [[Publisher](#)]
- [29]. Diallo A., Beye A.C., Doyle T.B., Park E., Maaza M. *Green Chem. Lett. Rev.*, 2015, **8**:30 [[Crossref](#)], [[Google Scholar](#)], [[Publisher](#)]
- [30]. Holt L.R., Plowman B.J., Young N.P., Tschulik K., Compton R.G. *Angew. Chem. Int. Ed.*, 2016, **55**:397 [[Crossref](#)], [[Google Scholar](#)], [[Publisher](#)]
- [31]. Ahmad F., Kainat K., Farooq U. . *J. Chem. Rev.*, 2022, **4**:374 [[Crossref](#)], [[Publisher](#)]
- [32]. Laviron E. *J. Electroanal. Chem.*, 1979, **101**:19 [[Crossref](#)], [[Google Scholar](#)], [[Publisher](#)]

How to cite this manuscript: B. Dhinakaran *, S. Monika, S. Nivetha, M. Shalini, B. Vishnupriya, K. Sathiyamoorthi. Sustainable Synthesis of Cobalt Nanoparticles from Temple Waste flowers of Pink Rose, Red Rose, Yellow Rose and Orange Rose Petals Extracts. *Asian Journal of Nanoscience and Materials*, 2023, 6(1), 53-68. DOI: 10.26655/AJNANOMAT.2023.1.4